J. Fluid Mech. (1978), *vol.* 84, *part* 2, *pp.* 281–290
Printed in Great Britain

Fluid flow in a hemisphere induced by a distributed source of current

By J. G. ANDREWS

Central Electricity Generating Board, Marchwood Engineering Laboratories, Southampton, England

AND R. E. CRAINE

Department of Mathematics, University of Southampton, England

(Received 20 December 1976 and in revised form 10 May 1977)

One of the main problems in welding is to produce consistent weld profiles. Simple heat-flow models of the weldpool, which are currently used to predict the shape of the solid–liquid boundary, do not take account of fluid motion which is observed in practice and the effect of such motion could be significant. Electromagnetic $\mathbf{j} \times \mathbf{B}$ forces due to the welding arc have been proposed as a major cause of the motion and we attempt here to develop existing flow models towards more practical welding situations. We consider the steady-state flow of an incompressible viscous conducting fluid in a hemispherical container due to various axisymmetric representations of the distributed current sources which can arise in arc welding. A solution is found for sufficiently small currents that inertial effects may be ignored and no singularities appear in the velocity field. We discover that varying the current distribution can lead to qualitatively different flow patterns, i.e. poloidal flows in opposite directions and breakup into two distinct counter-rotating loops.

1. Introduction

In recent years there has been considerable interest in understanding the physical mechanisms underlying welding processes. Fusion welding has received the most attention, both experimentally and theoretically. Heat-conduction models of the weldpool in fusion welding have been extensively investigated (Carslaw & Jaeger 1959; Rosenthal 1941; Christensen, Davies & Gjermundsen 1965) but recent experiments (Woods & Milner 1971; Kublanov & Erokhin 1974) have cast doubt on these models by demonstrating the presence of vigorous motion of the molten metal, which may substantially affect the shape of the solid–liquid boundary. These experiments have suggested that the electromagnetic $\mathbf{j} \times \mathbf{B}$ force due to the welding arc is the primary cause of the motion, where $\mathbf{j}$ is the current density and $\mathbf{B}$ is the magnetic induction.

Some theoretical attention has been given to this topic in the last few years, originating from the work of Shercliff (1970) on the flow of a semi-infinite inviscid conductor due to a stationary point source of current situated on the plane boundary. His solution contains singularities in the velocity field on the axis of symmetry. Sozou (1971) removed these singularities by adding viscosity to the model but when the

dimensionless parameter $K = \mu_0 \rho I^2/2\pi^2\eta^2$ exceeds 300·1 singularities in the velocity field again develop along the axis. In this expression I, μ_0, ρ and η are the total current of the discharge and the permeability, density and dynamic viscosity of the material, respectively, in mks units.

There have since been several extensions of the point-source model. Narain & Uberoi (1971, 1973) have modified the Shercliff and Sozou solutions to describe flow in a conical region. Sozou & English (1972) have included the effect of the back e.m.f. and Sozou (1974) has considered flow confined to a cone and a central column, both papers applying to a semi-infinite fluid region. The transient build-up to the steady-state problem in Sozou (1971) has been solved by Sozou & Pickering (1975) and the same authors have recently (1976) found the steady-state solution in a finite hemisphere. In all these extensions there remains a critical value K_{crit} of K above which the velocity field breaks down on the axis. K_{crit} varies to some extent from problem to problem, for instance $K_{\text{crit}} = 94{\cdot}1$ for a finite hemisphere with a free surface (Sozou & Pickering 1976). Taking typically quoted values for steel (Smithells 1967) of $\mu_0 = 4\pi \times 10^{-7}$, $\rho = 8 \times 10^3$ and $\eta = 10^{-3}$, we find that $K_{\text{crit}} = 94{\cdot}1$ leads to a maximum current of about $\frac{1}{2}$A, which is very low compared with the normal welding currents of several hundred amps. In all the papers mentioned above, the limiting currents which are allowed remain too low for practical welding conditions.

In practice, the current entering the material is distributed over a finite region and the singularity in the electromagnetic force $\mathbf{j} \times \mathbf{B}$, inherent in the point-source model, does not exist. It therefore seems possible that the singularities in the velocity field could be removed by considering a distributed source of current on the surface. It appears that the only published work on flow due to a distributed source is by Sozou (1972), who considered the far-field solution in a semi-infinite fluid, i.e. the region $r \gg a$, where a is the radius of his disk source of current. Experimental observation suggests, however, that in welding the area over which the current enters the surface is a significant proportion of the total area of the pool.

In this paper, therefore, we shall consider the steady-state flow of an incompressible fluid in a finite region due to a stationary distributed source and solve for the flow in the entire pool. For convenience, following Sozou & Pickering (1976), we restrict attention to a hemispherical pool of radius r_0 and employ spherical polar co-ordinates (r, θ, ϕ). The basic fluid equation to be solved is the steady-state momentum equation

$$\rho(\mathbf{v}.\nabla)\mathbf{v} = -\nabla p + \mathbf{j} \times \mathbf{B} - \eta \nabla \times \boldsymbol{\omega}, \tag{1}$$

where $\mathbf{v}$ is the velocity of the fluid, p is the static pressure and $\boldsymbol{\omega} = \nabla \times \mathbf{v}$ is the vorticity.

The first step in solving the above equation is to establish suitable self-consistent current distributions satisfying Maxwell's equations; these are obtained in §2. Using these current distributions, in §3 we look for solutions to the linearized problem, where the inertial term on the left-hand side of (1) is neglected. We then show in §5 that this neglect is always reasonable near the origin and for practical current distributions is also valid in the body of the fluid for currents up to 15 A. Results for various current distributions are presented in §4 and we discover that qualitatively different flow patterns can arise. The implications of these results are discussed in §5.

2. Current distributions

Ignoring the effect of the fluid motion on the current, the current density $\mathbf{j}$ will be given by Ohm's law

$$\mathbf{j} = -\sigma \nabla V, \tag{2}$$

where σ is the electrical conductivity and V is the electrostatic potential, which satisfies Laplace's equation $\nabla^2 V = 0$. The magnetic induction $\mathbf{B}$ is obtained from Maxwell's equation

$$\nabla \times \mathbf{B} = \mu_0 \mathbf{j}, \tag{3}$$

where μ_0 is the permeability.

One method of obtaining solutions to Laplace's equation is to construct potential distributions due to combinations of sources and sinks, and since this proves to be very convenient in representing the peaked current distributions on the surface of the pool due to a welding arc and in representing the current take-off points within the material, we shall adopt this approach here. Since the electrical conductivities of the arc, solid and liquid metal are significantly different, the model will not give an adequate physical description of the current distribution *above* the surface as the siting of the 'source' will not coincide with the source of current from the electrode. However, we emphasize that the use of sources and sinks does produce suitable representations of the current flow in the region of interest, which is *inside* the weldpool.

The simplest possible representation is that of a point source of current situated on the surface of a semi-infinite conducting material. This is the situation considered by a number of authors, including Shercliff (1970) and Sozou (1971), but in this model V, $\mathbf{j}$, $\mathbf{B}$ and $\mathbf{j} \times \mathbf{B}$ are all singular at $r = 0$.

In the practical welding situation the current density on the surface of the pool is everywhere finite and, furthermore, the current is tapped off from points situated a finite distance from the pool. Woods & Milner (1971) have shown experimentally that the positioning of the points where the current is tapped off significantly affects the direction of fluid flow in the pool. It is common welding practice to tap the current from points situated off the axis of symmetry, but for the present we restrict attention to axisymmetric distributions. A fairly simple model with the required physical features is that of a point source placed a distance a above the surface together with a ring sink of equal strength situated below the surface and centred on the axis of symmetry. The angle subtended by the ring is taken to be 2α and the radius of the ring to be $b \sin \alpha$. We note that when $\alpha = 0$ the ring sink becomes a point sink (on the axis of symmetry at a distance b below the surface) – an important special case of the general results.

Expressions in closed form for the potential due to a ring sink are not available but infinite series representations are well known (see, for example, Jeans 1925). Since the ring lies outside the molten pool we have $r < b$ for all points inside the pool and in this case the potential due to the ring sink is given by

$$V = -(I/4\pi\sigma b) \sum_{n=0}^{\infty} P_n(\cos\alpha)(r/b)^n P_n(\mu), \tag{4}$$

where $\mu = \cos\theta$ and P_n is the Legendre polynomial of degree n. The potential due to the point source above the surface is $V = (I/4\pi\sigma)(a^2 + r^2 + 2ar\mu)^{-\frac{1}{2}}$. In this paper we shall

consider only those representations in which $r_0 < a$, where r_0 denotes the radius of the pool, in which case we may express V for the point source as an infinite series of the form (4) with $P_n(\cos\alpha)$ replaced by $(-b/a)^{n+1}$. The combined potential due to the point source and ring sink may then be written as

$$V = -(I/4\pi\sigma r_0)\sum_{n=0}^{\infty} d_n R^n P_n(\mu), \tag{5}$$

where R and d_n are defined by

$$R = r/r_0, \quad d_n = (r_0/b)^{n+1} P_n(\cos\alpha) + (-r_0/a)^{n+1}, \tag{6a,b}$$

respectively. Substituting for V from (5) into (2) and (3) yields

$$\mathbf{j} = \frac{I}{4\pi r_0^2}\left(\sum_{n=1}^{\infty} d_n n R^{n-1} P_n(\mu), -(1-\mu^2)^{\frac{1}{2}}\sum_{n=1}^{\infty} d_n R^{n-1} P_n'(\mu), 0\right) \tag{7}$$

and

$$\mathbf{B} = \frac{\mu_0 I}{4\pi r_0}(1-\mu^2)^{\frac{1}{2}}\left(0, 0, \sum_{n=1}^{\infty} d_n R^n P_n'(\mu)/(n+1)\right), \tag{8}$$

where

$$P_n'(\mu) \equiv dP_n(\mu)/d\mu.$$

3. Fluid flow problem

3.1. *Basic equations*

We now consider the fluid flow problem in a finite hemisphere; there are natural similarities between our method and that of Sozou & Pickering (1976). We find it convenient to employ a non-dimensional stream function $\Psi = 4\rho\psi/K\eta r_0$ and the corresponding velocity $\mathbf{v}$ is

$$\mathbf{v} = -(\eta K/4\rho r_0)\{R^{-2}\partial\Psi/\partial\mu, R^{-1}(1-\mu^2)^{-\frac{1}{2}}\partial\Psi/\partial R, 0\}. \tag{9}$$

The complete set of boundary conditions to be satisfied is

$$\Psi = \partial^2\Psi/\partial\mu^2 = 0 \quad \text{on} \quad \mu = 0, \tag{10}$$

$$\Psi = \partial\Psi/\partial R = 0 \quad \text{on} \quad R = 1, \tag{11}$$

$$\Psi = 0, \quad \partial\Psi/\partial\mu, \quad (1-\mu^2)^{-\frac{1}{2}}\partial\Psi/\partial R \quad \text{both finite on } \mu = 1, \tag{12}$$

$$R^{-2}\partial\Psi/\partial\mu, \quad R^{-1}\partial\Psi/\partial R \quad \text{both finite as } R \to 0. \tag{13}$$

Equation (10) implies that the free surface of the pool is both flat and coincident with a streamline and that the shear stress is zero on this surface. Equation (11) represents the no-slip conditions on the liquid–solid interface. The requirements that the axis of symmetry be a streamline and that the velocity be finite both on the axis and at the origin are embodied in conditions (12) and (13).

The complete fluid flow problem requires the solution of (1) but after taking the curl to remove the conservative terms the resulting equation remains nonlinear owing to inertial effects and only numerical solutions seem feasible. In order to obtain some insight into the difference in character between the point-source solution (Sozou & Pickering 1976) and that for various distributed sources, it is instructive to obtain analytic solutions and we therefore restrict attention to the linear problem obtained when inertial effects are ignored.

3.2. *Linearized solution*

By taking the curl of (1), neglecting the inertia terms and using (7)–(9) it may be shown that the linearized equation is of the form

$$D^2\Psi = -\sum_{s=1}^{\infty} R^{s+1} F_s(\mu), \tag{14}$$

where D is the operator

$$D \equiv \partial^2/\partial R^2 + R^{-2}(1-\mu^2)\,\partial^2/\partial\mu^2. \tag{15}$$

In deriving the right-hand side of (14) it proves convenient to use the result

$$\operatorname{curl}(\mathbf{j}\times\mathbf{B}) = \hat{\boldsymbol{\phi}} 2B_\phi\{j_r + j_\theta\mu(1-\mu^2)^{-\frac{1}{2}}\}/r \tag{16}$$

(Shercliff 1970). In terms of cylindrical polar co-ordinates (ρ, θ, ϕ) the right-hand side of (16) can be written as $\hat{\boldsymbol{\phi}} 2B_\phi j_\rho/\rho$, and this simpler form is useful in discussing the flow patterns which occur in the weldpool (see §5). The functions $F_s(\mu)$, which arise from the appearance of Legendre polynomials in (7) and (8), are polynomials of degree $s+1$ (for further details concerning the results in this section the interested reader should consult Andrews & Craine 1977).

In general the polynomials $F_s(\mu)$ contain both odd and even terms. However, since our interests are restricted to the half-range $0 \leqslant \mu \leqslant 1$, we may express $F_s(\mu)$ in this region as an odd series by defining a suitable extension of the function in the range $-1 \leqslant \mu \leqslant 0$. It proves appropriate to write

$$F_s(\mu) = \sum_{n=1}^{\infty} \gamma_{2n}^{(s)}(1-\mu^2)\,P'_{2n}(\mu), \tag{17}$$

from which it follows that

$$\gamma_{2n}^{(s)} = \frac{(4n+1)}{2n(2n+1)}\int_0^1 F_s(\mu)\,P'_{2n}(\mu)\,d\mu. \tag{18}$$

Since a particular integral of the equation

$$D^2\Psi_s = -\gamma_{2n}^{(s)} R^{s+1}(1-\mu^2)\,P'_{2n} \tag{19}$$

is

$$\Psi_s = -h_{2n}^{(s)} R^{s+5}(1-\mu^2)\,P'_{2n}, \tag{20}$$

where the coefficient $h_{2n}^{(s)}$ is given by

$$h_{2n}^{(s)} = \gamma_{2n}^{(s)}/\{2n(2n+1)-(s+5)(s+4)\}\{2n(2n+1)-(s+3)(s+2)\}, \tag{21}$$

the solution of (14) is

$$\Psi = \sum_{n=1}^{\infty}\left\{a_{2n}R^{2n+1} + b_{2n}R^{2n+3} - \sum_{s=1}^{\infty} h_{2n}^{(s)} R^{s+5}\right\}(1-\mu^2)\,P'_{2n}(\mu). \tag{22}$$

The only boundary condition from the set (10)–(13) still to be satisfied is (11), i.e. $\Psi = \partial\Psi/\partial R = 0$ on $R = 1$, from which the unknown coefficients a_{2n} and b_{2n} can easily be obtained since the $P'_{2n}(\mu)$ form an orthogonal set of functions with respect to the weighting factor $(1-\mu^2)^{\frac{1}{2}}$. The complete solution to our linearized problem is then

$$\Psi = \sum_{n=1}^{\infty}\sum_{s=1}^{\infty}\{(n-\tfrac{1}{2}s-1)\,R^{2n+1} - (n-\tfrac{1}{2}s-2)\,R^{2n+3} - R^{s+5}\}\,h_{2n}^{(s)}(1-\mu^2)\,P'_{2n}(\mu). \tag{23}$$

We emphasize that the $h_{2n}^{(s)}$ depend only on the form of the current distribution in the material. Table 1 lists the coefficients $h_{2n}^{(s)}$ for particular current distributions of interest.

	$a/b = 1, \alpha = 0$				$a/b = \frac{1}{2}, \alpha = 0$			
s	$n = 1$	$n = 2$	$n = 3$	$n = 4$	$n = 1$	$n = 2$	$n = 3$	$n = 4$
1	0	0	0	0	−7·41	−4·00	−0·48	−0·05
2	6·20	0	0	0	2·84	0	0	0
3	0	0	0	0	−0·72	−1·44	−0·88	−0·12
4	0·28	1·12	0	0	0·16	0·52	0	0
5	0	0	0	0	−0·04	−0·15	−0·27	−0·18
6	0·03	0·07	0·21	0	0·02	0·04	0·10	0

	$a/b = \frac{3}{4}, \alpha = 0$				$a/b = \frac{3}{4}, \alpha = 0{\cdot}1\pi$			
s	$n = 1$	$n = 2$	$n = 3$	$n = 4$	$n = 1$	$n = 2$	$n = 3$	$n = 4$
1	−6·13	−3·31	−0·40	0·04	−6·65	−3·59	−0·43	0·04
2	3·53	0	0	0	2·96	0	0	0
3	−0·63	−1·31	−0·81	−0·11	−0·70	−1·54	−0·97	−0·13
4	0·16	0·60	0	0	0·17	0·56	0	0
5	−0·04	−0·14	−0·26	−0·18	−0·04	−0·14	−0·29	−0·19
6	0·02	0·04	0·11	0	0·02	0·04	0·10	0

TABLE 1. Coefficients $10^5\, h_{2n}^{(s)}$ for various current distributions.

4. Results

4.1. *Point source and sink on axis*

We now consider particular solutions (23) for a number of current distributions of the types described in § 2. As stated earlier, the siting of the source has no direct physical significance. Furthermore, since we are interested here only in the broad qualitative features of the possible flows that may arise, in our numerical computations we choose values of a and b which are fairly representative of real welding conditions and lead to interesting results. We examine first the distribution due to a point source and point sink both situated on the axis of symmetry.

When the source and sink are equidistant from the surface of the pool the infinite-series representation of their combined potential, given by (5) with $\alpha = 0$ and $a = b$, contains odd powers of R only since $d_{2n} \equiv 0$. This leads to correspondingly simple forms for $\mathbf{j} \times \mathbf{B}$ and the stream function, as can be seen from the coefficients $h_{2n}^{(s)}$ displayed in table 1. The leading non-zero term ($n = 1$, $s = 2$) in (23) is

$$\Psi = -3h_2^{(2)} R^3 (1 - R^2)^2 \mu (1 - \mu^2), \tag{24}$$

where $h_2^{(2)} = 6{\cdot}20 \times 10^{-5}$. Inspection of the magnitudes of the higher coefficients $h_{2n}^{(s)}$ listed in table 1 suggests that convergence may be slow. However, (24) provides a fair approximation to the stream function over most of the pool, as may be found from either the numerical evaluation of (23) or a closer analysis of the higher terms, whose radial dependence is governed by both the general form of the solution and the boundary conditions at $R = 0$ and $R = 1$.

Figure 1 (*a*) shows the streamlines for the case $a = b$. In this example and all subsequent ones, the ratio r_0/a is assumed to be 0·5. Sufficient terms have been included to restrict the numerical error in this example (and all subsequent examples) to around 1 %; the number of terms used is indicated on each graph. Greater accuracy is considered unnecessary since we wish to show only the broad features of the flow for various

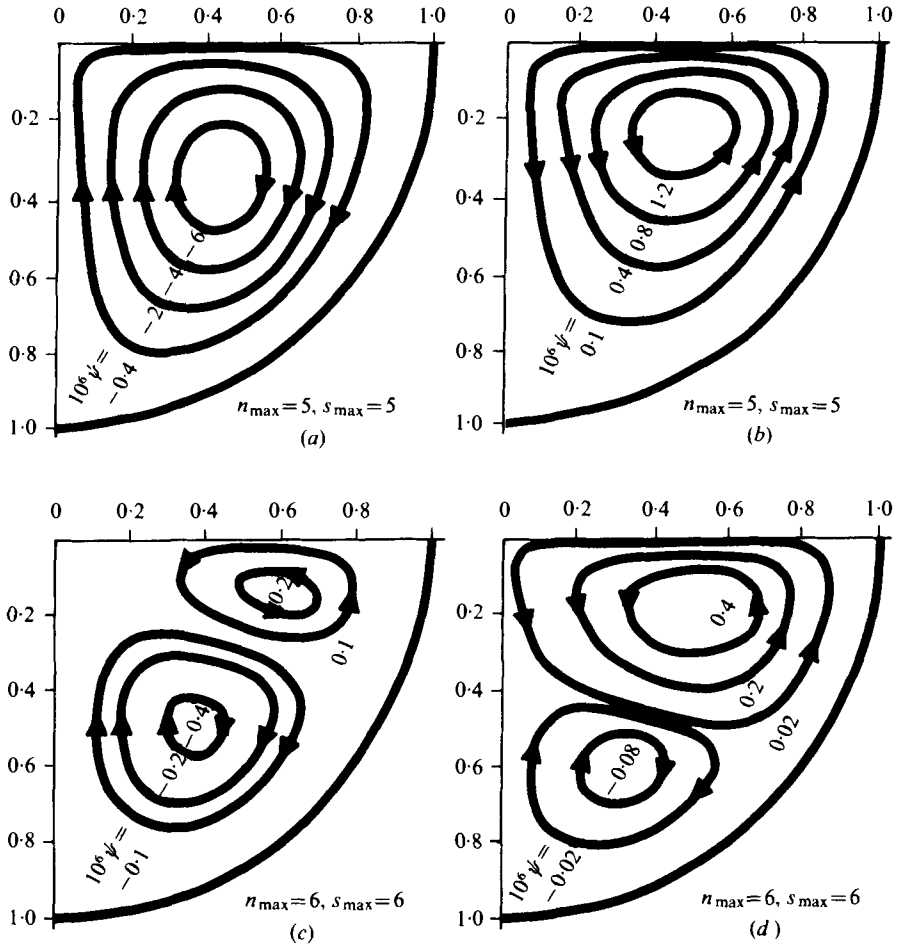

FIGURE 1. Cross-sections of flows due to a point source and a sink. (*a*) $a/b = 1$, $\alpha = 0$; (*b*) $a/b = \frac{1}{2}$, $\alpha = 0$; (*c*) $a/b = \frac{3}{4}$, $\alpha = 0$; (*d*) $a/b = \frac{3}{4}$, $\alpha = 0{\cdot}1\pi$.

types of current distribution. The direction of the flow is indicated on the diagram and it is interesting to note that the flow is radially outwards on the surface, i.e. in the *opposite* sense to that for a point source of current on the surface (Sozou & Pickering 1976). Also, the flow pattern close to the origin does not seem to indicate a singularity. This point is discussed further in §5.

The effect of the position of the point sink on the motion was investigated for a number of values of a/b. A transition takes place as this ratio is decreased from $a/b = 1$ to $a/b = 0{\cdot}5$: from radially outward flow on the surface (figure 1*a*) to radially inward flow (figure 1*b*). In the transition region the flow pattern breaks up into two separate regions, as shown in figure 1(*c*). This figure demonstrates the interesting result that there can be radially inward flow on the surface but motion in the opposite sense in the bulk of the molten region. The fact that the direction of rotation reverts to that in the point-source problem (Sozou & Pickering 1976) as a/b decreases is not surprising since the contribution due to the point sink diminishes as b increases, leaving the point source above the surface to dominate in the pool.

Kublanov & Erokhin (1974) have confirmed experimentally the general direction of flow predicted by Sozou & Pickering for a fairly concentrated source of current in a large (100 mm diameter) hemispherical bowl of gallium. Experiments under more typical welding conditions are in progress (Willgoss 1977, private communication) on the effect of varying the current distribution along the lines discussed in this paper.

4.2. *Point source and ring sink*

The other main type of current distribution examined earlier was that due to a point source and a ring sink centred on the axis of symmetry. Solutions (23) have been evaluated for a large number of values of α and a/b. The results are qualitatively similar to those discussed in §4.1.

As stated earlier, the ring sink degenerates to a point sink on the axis of symmetry as $\alpha \to 0$. For small values of α we should therefore expect the flow pattern for the ring sink to be closely related to that for the corresponding point sink. We illustrate this point for $\alpha = 0{\cdot}1\pi$ and $a/b = 0{\cdot}75$ in figure 1(*d*), which shows a double-loop system similar to that in figure 1(*c*), although we observe that the upper loop has now become dominant. Indeed as α is increased further our results indicate that the lower loop disappears completely.

With the ring sink situated on the upper surface of the material, i.e. $\alpha = \frac{1}{2}\pi$, the solution (23) was evaluated for a number of ratios a/b and in all cases was found to produce only a single loop with radially inward flow on the surface. The flow patterns looked similar to those shown in figure 1(*b*) and are not reproduced.

5. Discussion

As mentioned in the introduction, the point-source model examined by previous workers leads to an inherent singularity in the velocity field near the origin, and further singularities in the velocity near the origin in the nonlinear problem when $K > K_{\text{crit}}$. However, for the current distributions considered here we have found a velocity field for the linearized problem which tends to zero at the origin, as can be seen from (9) and (23). That the origin should be a stagnation point in our case is not surprising since $\mathbf{j} \times \mathbf{B}$ and $\nabla \times (\mathbf{j} \times \mathbf{B})$ both vanish there. Moreover, for our distributed model we should not expect inertial effects to play a significant role in this region. This is confirmed by using the linearized solution to evaluate the leading terms in (1), since one finds in all cases that the R dependence is of a lower order for the viscous and forcing terms than for the inertial term. Indeed, taking the limit as $R \to 0$ of the nonlinear equation (cf. Sozou & Pickering 1976), we can deduce that $\Psi \to 0$ and that there are no singularities in the velocity field corresponding to those found for the point-source model. Therefore, by considering a distributed source of current we have eliminated the breakdown of the velocity field near the origin inherent in the point-source model.

Nevertheless, in the body of the fluid the linearized solution is valid only for small Reynolds numbers and it is of interest to estimate the maximum currents which are thereby permissible. We have calculated the ratio of the inertial to the forcing terms in (1) at a large number of points in the pool for the various distributions discussed in §4. In each case we find that the ratio is small compared with unity (say, 0·3) provided

that the current does not exceed some value between 5 and 15 A. We assumed the values of the material constants quoted in the introduction and put $a = 5$ mm, which leads to a power distribution on the surface of the pool typical of that observed in practice. This clearly represents a significant advance on the limit to the current of around 1 A, found by Sozou & Pickering (1976), for the point-source model. However, normal welding currents are several hundred amps and a nonlinear distributed source model would be needed to cope with this regime.

It is important to note that the directions of fluid flow could have been predicted from the sign of the right-hand side of (16). For our axisymmetric current distributions B_ϕ is always one-signed and therefore the sign of the radial current flow, j_ρ, in cylindrical polars determines the sign of curl $(\mathbf{j} \times \mathbf{B})$ in the weldpool and hence controls the direction of fluid flow. It is easy to see that, for the current distributions leading to figures 1 (*a*)–(*d*), j_ρ is always negative in the weldpool in figure 1 (*a*), always positive in the pool for figure 1 (*b*) and changes sign within the pool in the remaining two cases. Shercliff (1970) has argued that a positive j_ρ leads to inward flow of fluid on the top surface. Since a negative j_ρ results in outward flow of fluid the flow patterns displayed in figure 1 are in full qualitative agreement with those suggested by the current distribution in the weldpool.

It should be remembered that the numerical results in §4 have been evaluated for one particular value of the ratio r_0/a, i.e. $r_0/a = 0{\cdot}5$. Clearly the flow patterns vary as r_0/a is changed but further numerical results are not quoted here since no new qualitative phenomena arise. The recent numerical results of Atthey (1977, private communication), who solves the full nonlinear problem using a numerical method based on finite differences, confirm this view.

The practical importance of fluid convection in the weld pool is that it affects the shape of the solid–liquid boundary. The low Reynolds number solution obtained here leads to Péclet numbers (i.e. characteristic ratio of heat convection to heat conduction) which are of order 10^{-1} and so we do not expect convection significantly to alter the position of the boundary. Nevertheless, it is worth noting that radially outward fluid flow on the surface should produce shallower pools whereas radially inward flow should deepen the pool.

Finally, we emphasize that all our solutions are axisymmetric. In practice, asymmetries are usually present through both the tapping of the current from one side of the pool and the traversing motion of the workpiece relative to the arc. These asymmetries might lead to yet further varieties of flow pattern and they will form the subject of future investigations.

The authors are indebted to Mr A. J. Shrapnel for performing the numerical computations and to the referees for some helpful comments.

REFERENCES

Andrews, J. G. & Craine, R. E. 1977 *C.E.G.B. Lab. Note* R/M/N919.

Carslaw, H. S. & Jaeger, J. C. 1959 *Conduction of Heat in Solids*, 2nd edn. Oxford: Clarendon Press.

Christensen, N., Davies, V. de L. & Gjermundsen, K. 1965 *Br. Weld. J.* **12**, 54.

Jeans, J. 1925 *The Mathematical Theory of Electricity and Magnetism*, 5th edn, p. 226. Cambridge University Press.

KUBLANOV, V. & EROKHIN, A. 1974 *Int. Inst. Weld. Doc.* no. 212-318-74.
NARAIN, J. P. & UBEROI, M. S. 1971 *Phys. Fluids* **14**, 2687.
NARAIN, J. P. & UBEROI, M. S. 1973 *Phys. Fluids* **16**, 940.
ROSENTHAL, D. 1941 *Weld. J. Easton* **20**, 220S.
SHERCLIFF, J. A. 1970 *J. Fluid Mech.* **40**, 241.
SMITHELLS, C. J. 1967 *Metals Reference Book*, vol. 3. Butterworths.
SOZOU, C. 1971 *J. Fluid Mech.* **46**, 25.
SOZOU, C. 1972 *Phys. Fluids* **15**, 272.
SOZOU, C. 1974 *J. Fluid Mech.* **63**, 665.
SOZOU, C. & ENGLISH, H. 1972 *Proc. Roy. Soc.* A **329**, 71.
SOZOU, C. & PICKERING, W. M. 1975 *J. Fluid Mech.* **70**, 509.
SOZOU, C. & PICKERING, W. M. 1976 *J. Fluid Mech.* **73**, 641.
WOODS, R. A. & MILNER, D. R. 1971 *Weld. J. Res. Suppl.* **50**, 163S.